Journal of Chromatography A, 1437 (2016) 88–94

Contents lists available at ScienceDirect

Journal of Chromatography A

journal homepage: www.elsevier.com/locate/chroma

Chiral separation by a terminal chirality triggered *P*-helical quinoline oligoamide foldamer

Hiroki Noguchi[a,b,c], Makoto Takafuji[a], Victor Maurizot[b,c], Ivan Huc[b,c,**], Hirotaka Ihara[a,d,*]

[a] Department of Applied Chemistry and Biochemistry, Kumamoto University, 2-39-1 Chuoku, Kurokami, Kumamoto 860-8555, Japan
[b] University of Bordeaux, CBMN (UMR 5248), Institut Européen de Chimie Biologie, 2 rue Escarpit, 33600 Pessac, France
[c] CNRS, CBMN (UMR 5248), 2 rue Escarpit, 33600 Pessac, France
[d] Kumamoto Institute for Photo-electro Organics (PHOENICS), 3-11-38 Higashimachi, Kumamoto, Japan

ARTICLE INFO

Article history:
Received 18 November 2015
Received in revised form 26 January 2016
Accepted 26 January 2016
Available online 1 February 2016

Keywords:
Chiral stationary phase
Enantioselectivity
Helical structure
Aromatic foldamers
Chiral HPLC

ABSTRACT

A *P*-helical quinoline oligoamide foldamer was grafted on silica and applied as an HPLC stationary phase for chiral separation. The *P*-handedness of the quinoline oligoamide foldamer was induced by a (1*S*)-camphanyl group, which was introduced at the N-terminus of a tetrameric quinoline oligoamide foldamer (Cmp-Q_4). To immobilize the foldamer on porous silica particles, a trimethoxysilyl group was introduced at the opposing end of the foldamer. Elemental analysis indicated that the amount of foldamer on the silica surface was 0.57 μmol/m^2. Circular dichroism and vibrational CD spectra of Cmp-Q_4 and Cmp-Q_4-immobilized silica (Sil-Q_4-Cmp) suggested that the helical structure of Cmp-Q_4 was altered on the silica surface whilst retaining a chiral structure. The chiral recognition ability of Sil-Q_4-Cmp was evaluated with various aromatic enantiomers. Sil-Q_4-Cmp showed enantio-selectivity for axially chiral molecules (e.g., $\alpha_{\text{Trigger's base}} = 1.26$ and $\alpha_{\text{Binaphthol}} = 1.07$). Sil-$Q_4$-Cmp showed remarkable recognition of helical octameric quinoline oligoamides with isobutoxy and triethylene glycol side chains ($\alpha = 10.35$ and 14.98, respectively). In contrast, an (1*S*)-camphanyl group-immobilized porous silica showed no chiral recognition for any enantiomers tested in this study. To elucidate the chiral separation mechanism of Sil-Q_4-Cmp, thermodynamic parameters were calculated using van't Hoff plots. HPLC results and thermodynamic parameters suggested that the chiral recognition of Sil-Q_4-Cmp is based on the helical structure of Cmp-Q_4 and other thermally dependent interactions such as hydrophobic effects associated with aromatic stacking. This work represents the first known application of aromatic foldamers in chiral separation.

1. Introduction

Enantiomers of chiral molecules show different physiological activities. For their applications in various fields including pharmaceuticals, perfumes [1], foodstuffs [2], and pesticides [3], analytical and separation techniques allowing to discrimination and purification enantiomers are important tools. In particular, more than half of all pharmaceutical products are chiral molecules having a defined absolute stereochemistry [4] and whose wrong enantiomer may have undesirable effects; in those cases, precise analytical techniques are essential. Among the various techniques used, high-performance liquid chromatography (HPLC) is widely utilized as it is fast, highly sensitive, and versatile. Chiral HPLC, which allows the separation of enantiomers, can be divided into two methods: one uses diastereomerism, viz. converting enantiomers into diastereomers through covalent or ionic bonds to facilitate separation [5,6], whereas the other uses a chiral stationary phase (CSP), in which chiral molecules are directly bonded to a substrate such as porous silica particles to enable the direct recognition and discrimination of enantiomers in the mobile phase. The second method allows a direct separation of the enantiomers, thus circumventing pre- and post-treatments and simplifying the process. Despite seeing major progress in the technology, not all enantiomeric pairs can be conveniently separated with existing CSPs, and the development of highly selective CSPs with broad applicability is still needed. According to recent reports, a majority of CSPs use polysaccharide deriva-

* Corresponding author at: Kumamoto University, Department of Applied Chemistry and Biochemistry, 2-39-1 Kurokami, Kumamoto 860-8555, Japan. Fax: +81 96 342 3662.
** Corresponding author at: CNRS, CBMN (UMR 5248), 2 rue Escarpit, Pessac 33600, France. Fax: +33 540 002 215.
E-mail addresses: i.huc@iecb.u-bordeaux.fr (I. Huc), ihara@kumamoto-u.ac.jp (H. Ihara).

http://dx.doi.org/10.1016/j.chroma.2016.01.059
0021-9673/

tives such as amylose and cellulose [7], which have been proven to be useful. Various CSPs, including those using crown ethers and cyclodextrins [8,9], biomolecules such as proteins and glycopeptides [10,11], low molecular weight chiral molecules [12–14], and polymers with a chiral stereostructure [15,16], have been developed.

In recent years, there have been noticeable developments in the application of artificial helical polymers [17] and there is a significant interest in CSPs that use polymers with ordered chiral structures. The use of helical polymers as Chiral HPLC stationary phase necessitates a molecular design that maintains their chirality and helical structure in the mobile phase. For example, CSPs that use helical polymers consisting of polyamino acids [18] and helical polymers with chiral molecules in the side chain [19] have been reported. A remarkable example of a CSP demonstrating reversibly switchable enantioseparation based on helical polyacetylene was also reported [20]. Currently, research on foldamers, whose molecules can be folded into a helix, is being actively conducted [21–24]. Foldamers are synthetic oligomers that mimic the folding that occurs in the secondary structures of biomolecules such as proteins and peptides. Foldamers spontaneously fold in solution and may adopt diverse secondary structures with helices being the most common motif, stabilized through non-covalent interactions such as intramolecular hydrogen bonds, steric effects, and solvophobic forces. Depending on their chemical nature and length, foldamer conformations may be more or less stable, as well as solvent dependent. As far as we know, foldamer helicity has not been exploited in CSPs.

We have been conducting research on foldamers consisting of oligoamides of 8-amino-2-quinolinecarboxylic acid as the main chain (Q_n). In these oligomers, intramolecular hydrogen bonding between the amide groups and the endocyclic nitrogen atoms of neighboring quinoline rings, electrostatic repulsions between the amide carbonyl groups and the quinoline nitrogen atoms, and aromatic ring stacking, lead to the formation of a helical structure having 2.5 units per turn and a helix pitch (vertical rise per turn) of 3.5 Å in both solution and solid state [25–27]. These helices show outstanding conformational stability. For example, an octamer is still folded in DMSO at 120 °C [26]. In addition, although folding varies with solvent, the structure remains intact in all solvents tested: apolar, polar, aprotic, or protic [28]. Q backbones do not contain any stereogenic centers and thus, exist as a racemic mixture of *P*- and *M*-helices. However, the equilibrium between these conformational enantiomers can be quantitatively biased (based on NMR detection) in favor of either *P* or *M* helicity, influenced by an appended chiral group at one end of the helix (e.g., a camphanyl group at the N-terminus) [29,30]. In this study, we have immobilized a *P*-helical tetrameric quinoline oligoamide foldamer on the surface of porous silica particles as a new CSP and evaluated its ability to separate various pairs of enantiomers. Our results show that the new CSP does not have broad applicability. It shows moderate efficiency in some cases but, remarkably, a very high separation factor (α as large as 15) of helical (Q_n) oligomers was observed. The new CSP thus proved very efficient at separating foldamer helices that are similar to those attached to the silica. The *P*-enantiomers, which have the same handedness as those on the silica, showed slower elution that indicated preferred helix–helix interactions.

2. Experimental

2.1. Preparation of quinoline oligoamide and camphanic group-immobilized stationary phases

The quinoline oligoamide tetramer with 4-isobutoxy solubilizing chains and a (1*S*)-camphanyl N-terminal group (Cmp-Q_4), and a methyl ester at the C-terminus was synthesized according to previous reports [25,29]. The methyl ester function was saponified to produce a carboxylic acid, which was converted to the corresponding carboxylic acid chloride. A mono-Boc-protected diamine was introduced at the C-terminus via a coupling procedure using mono-*N*-Boc protected 1,3-diaminopropane. Deprotection of the Boc group was achieved using trifluoroacetic acid (TFA). Subsequently, 3-(triethoxysilyl)-propyl isocyanate was reacted with the resulting amine to form a urea. Cmp-Q_4 with its trimethoxysilyl group was immobilized on porous silica particles (YMC silica gel, 5 μm diameter, pore size 120 Å, surface area 330 m^2/g) in toluene under reflux conditions for 72 h. The functionalized silica is noted as Sil-Q_4-Cmp.

As a reference, the (1*S*)-camphanyl group was directly immobilized on porous silica particles (Sil-Cmp). Thus, 3-aminopropyltrimethoxysilane (APS) grafted silica (Sil-APS) was prepared by refluxing porous silica particles and APS in toluene for 24 h. Next, camphanyl chloride was coupled to the amino groups of Sil-APS in toluene at 60 °C for 24 h. Both Sil-Q_4-Cmp and Sil-Cmp were washed with hot toluene and chloroform several times and dried in vacuo (Fig. 1).

2.2. ^1H and ^{13}C NMR spectroscopy

^1H and ^{13}C nuclear magnetic resonance (NMR) spectra were recorded on Bruker Avance 300 (Bruker, USA) operating at 300 MHz for ^1H and 75 MHz for ^{13}C NMR. Chemical shifts were expressed in parts per million (ppm) using tetramethylsilane as an internal standard.

2.3. Elemental analyses, FT-IR, and DRIFT

Elemental analyses were carried out on a MICRO CORDER JM10 (J-Science Lab Co., Ltd., Kyoto, Japan). Fourier Transform Infrared (FT-IR) spectroscopy measurements were conducted on FT/IR-4100 (JASCO, Japan). For the Diffuse Reflectance Infrared Fourier Transform (DRIFT) measurement, the DR PRO410-M accessory (JASCO, Japan) was used.

2.4. UV–vis, CD, and VCD spectra

A Cmp-Q_4 chloroform solution (0.01 mM) and a Sil-Q_4-Cmp dispersion (0.1 mM) were prepared for the ultraviolet–visible (UV–vis) absorption and circular dichroism (CD) measurement. The concentration of Sil-Q_4-Cmp was calculated from their immobilized amount according to the elemental analysis result. UV–vis absorption were measured on the V560 spectrophotometer (JASCO Co., Ltd., Tokyo, Japan) while CD spectra were recorded on the J725 spectropolarimeter (JASCO Co., Ltd., Tokyo, Japan). A quartz cell of 1 cm optical path length was used. The Vibrational Circular Dichroism Spectra (VCD) were recorded using a VFT-4000 attachment.

2.5. Liquid chromatography

Sil-Q_4-Cmp and Sil-Cmp were packed into stainless-steel columns (150 × 4.6 mm i.d.). A JASCO 980 pump with a 'Rheodyne Model 7725 injector (10 μL loop), a JASCO MD-2010 plus multiwavelength detector, and a JASCO CD-2095 plus chiral detector were used for HPLC measurements. The column temperature was maintained using a column jacket with a heating and cooling system. A personal computer connected to the detector and pump, equipped with the ChromNAV (version 1.14) software, was used for system control and data analysis. Chromatographic grade solvents purchased from Nacalai Tesque, Inc. (Kyoto, Japan) were used to prepare the mobile phase and HPLC samples. The separation factor (α) was given by the ratio of retention factors (k). The retention

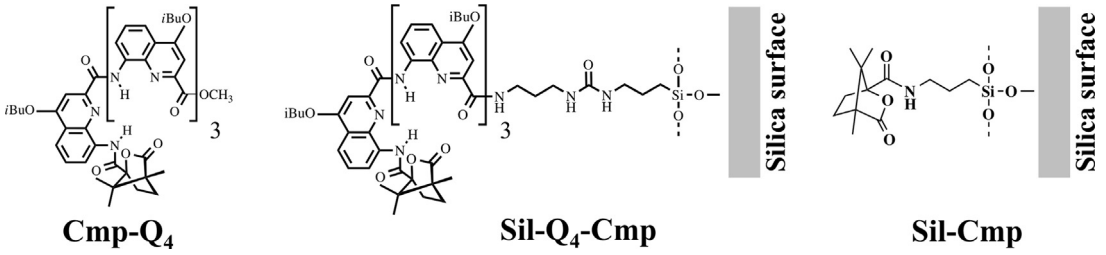

Fig. 1. Chemical structure of quinoline oligoamide (Cmp-Q_4), quinoline oligoamide and camphanic group immobilized stationary phases (Sil-Q_4-Cmp, Sil-Cmp).

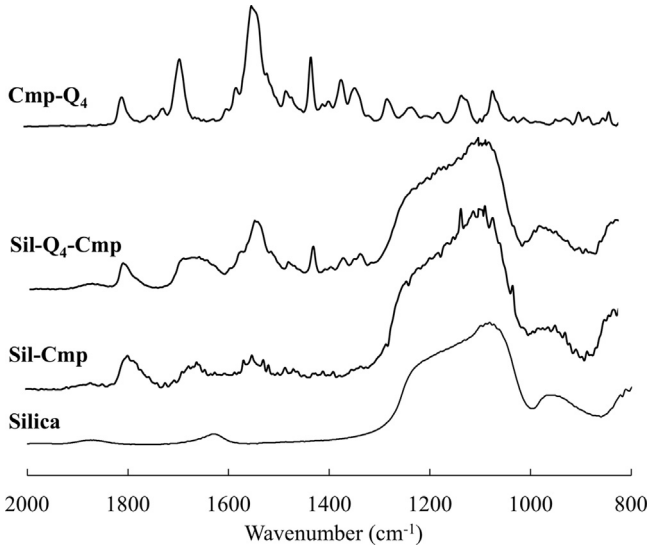

Fig. 2. Comparison of DRIFT spectra of Cmp-Q_4, Sil-Q_4-Cmp, Sil-Cmp and bare silica.

time of methanol was used as the void volume (t_0) marker (the absorption for methanol was measured at 220 nm).

3. Results and discussion

3.1. Immobilization of foldamer on the silica surface

Immobilization of Cmp-Q_4 onto porous silica particles was evaluated using IR-spectroscopy and elemental analysis. Fig. 2 shows the FT-IR spectra of Cmp-Q_4, Sil-Q_4-Cmp, Sil-Cmp, and unmodified porous silica. In the IR spectrum of Sil-Q_4-Cmp, new absorption bands, with respect to unmodified porous silica, corresponding to C=O stretching (1800 cm^{-1}) of the camphanyl group, C=C stretching of the quinoline ring (1536 cm^{-1}), and C=O stretching (1685 cm^{-1}) of the amide bond in the main chain were observed and they are characteristic absorptions of Cmp-Q_4. N–H bending of the amide bonds was postulated to overlap with the absorption peak at 1536 cm^{-1}. Based on these results, we concluded that Cmp-Q_4 was successfully immobilized on the silica particle surface in Sil-Q_4-Cmp. In addition, the IR spectrum of Sil-Cmp showed absorption bands originating from the C=O stretching of the camphanyl group at 1800 cm^{-1} and the C=O stretching of the amide group at 1644 cm^{-1}, inferring the generation of a stationary phase with only the camphanyl groups (without the foldamer). The elemental analysis results for Sil-Q_4-Cmp are shown in Table 1. The amount of immobilized Cmp-Q_4 was calculated using Eq. (1) [31] as shown below:

$$N(\mu mol/m^2) = \frac{10^6 P_c}{[1200 n_c - P_c M]S} \quad (1)$$

where P_c is the percentage of carbon based on the results of the elemental analysis, S is the specific surface area (330 m^2/g) of the porous silica particles used for immobilization, n_c is the number of carbons in one immobilized molecule, and M is the molecular weight of the molecules used for immobilization. The results showed that the immobilized amount of Cmp-Q_4 in Sil-Q_4-Cmp was 0.57 $\mu mol/m^2$. Similarly, the immobilized amount of Cmp in Sil-Cmp was found to be 1.31 $\mu mol/m^2$. The latter thus contains substantially more camphanyl groups, but without the foldamer helix.

3.2. Stereostructure of the foldamer before and after immobilization

The quinoline oligoamide foldamer with a (1*S*)-camphanyl group introduced at the N-terminus has been confirmed to possess a *P*-helical structure [29]. In a quinolinecarboxamide oligomer as short as a tetramer, an equilibrium between *P* and *M* helical conformers is rapidly obtained, with a characteristic time in the order of 100 ms [32,33]; leading to coalescence of some ^{1}H NMR diastereotopic signals [34]. In the case of Cmp-Q_4, the equilibrium should, in principle, be achieved in an equally fast measure but showed a complete bias in favor of the *P* helix instead and no *M* helix was detected. Neither the helical conformation nor the observed bias toward the *P* helix were altered upon heating to 50 °C in $CHCl_3$ and 100 °C in DMSO [see supporting information].

To confirm the stereostructure of the foldamer after immobilization onto the silica particle surface, we obtained its CD spectrum in a chloroform suspension and its VCD spectrum in the solid state. In the VCD spectrum of Cmp-Q_4, three positive peaks were observed at 1800 cm^{-1}, 1685 cm^{-1}, and 1539 cm^{-1}. These peaks corresponded to the absorption peaks of the C=O stretching (camphanyl group), the C=O stretching (amide bond), as well as the C=C stretching (quinoline ring) and the N-H bending (amide bond) in the IR spectrum, respectively. In the VCD spectrum of Sil-Q_4-Cmp, the C=O stretching of the amide bond was detected at a similar wavelength region as that of Cmp-Q_4, along with positive peaks at wavelengths corresponding to the C=C stretching of the quinoline ring and the N-H bending (Fig. 3). In addition, the peak intensity ratio at 1539 cm^{-1} and 1685 cm^{-1} ($\Delta Abs_{1539}/\Delta Abs_{1685}$) before and after immobilization was compared. While the peak intensity ratio before immobilization was 5.17, it became 2.33 after immobilization, i.e., it was reduced to about half. These results indicated that the amide site and the quinoline ring still retained a chiral arrangement after immobilization but with different structures. Fig. 4 shows the UV–vis absorption and CD spectra of Cmp-Q_4 and Sil-Q_4-Cmp. In the UV–vis spectrum of Cmp-Q_4 before immobilization, the absorption bands of the quinoline rings were observed at 327 and 358 nm. These bands were subsequently red-shifted to 337 and 374 nm, respectively, after immobilization.

The CD spectrum of Cmp-Q_4 featured positive peaks at 253, 309, 386, and 403 nm, consistent with a *P*-helical structure induced by the terminal (1*S*)-camphanyl group [29]. However, in Sil-Q_4-Cmp, a peak at 411 nm suggested a change in structure after immobiliza-

Table 1
Elemental analysis data and calculated immobilized amount of Sil-Q_4-Cmp.

		H%	C%	N%	C/N	Surface coverage [μmol/m^2]
Sil-Q_4-Cmp	Found	1.60	13.26	2.38	5.58	0.57
	Calcd.	1.11	13.26	2.33	5.69	

Surface coverage was calculated from C73H84N11O12Si for Sil-Q_4-Cmp.

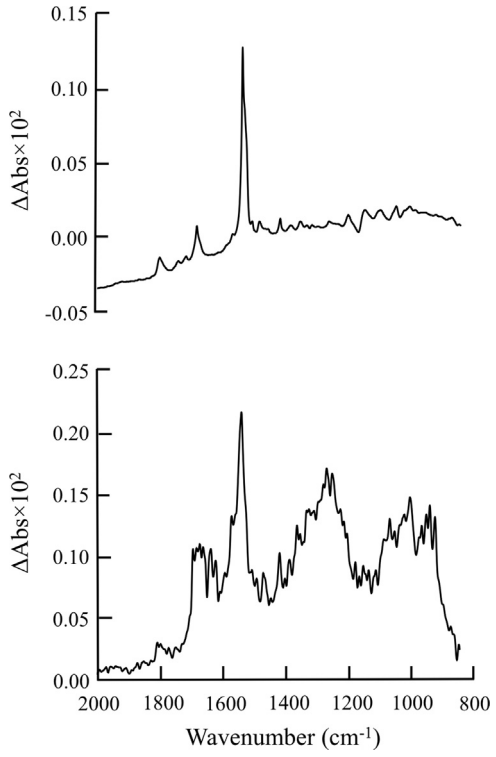

Fig. 3. Comparison of VCD spectrum of Sil-Q_4-Cmp (top) and Cmp-Q_4 (bottom).

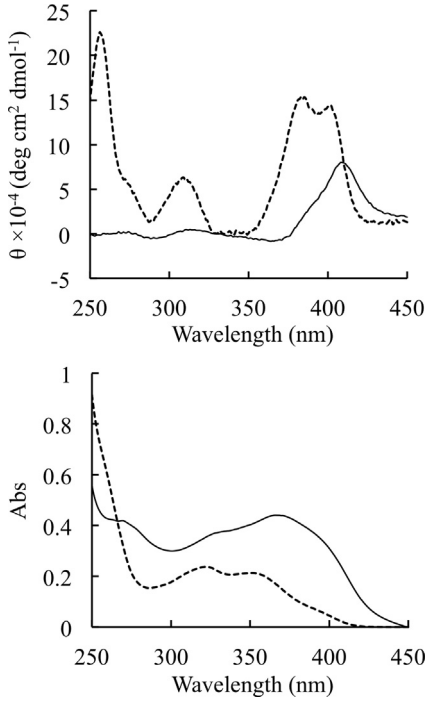

Fig. 4. CD Spectra (top) and UV spectra (bottom) of solution and suspended solution of Cmp-Q_4 (dotted line, 0.01 mM) and Sil-Q_4-Cmp (solid line, 0.1 mM) in $CHCl_3$.

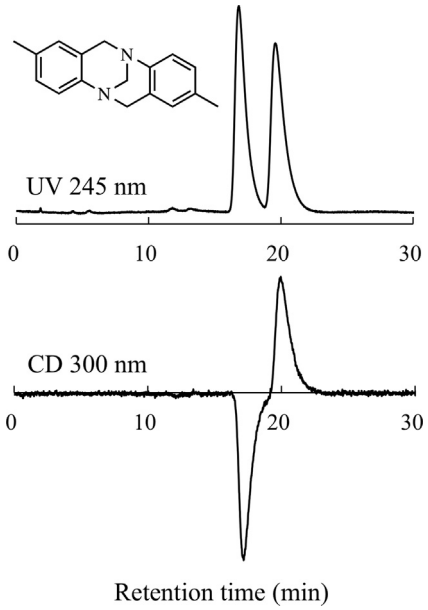

Fig. 5. Chromatograms of Troger's base on Sil-Q_4-Cmp. Mobile phase: methanol/water = 5/5, column temperature: 25 °C, flow rate: 1.0 ml min^{-1}, UV wavelength: 245 nm, CD wavelength: 300 nm.

tion. In summary, VCD, UV, and CD spectra indicated that Cmp-Q_4 maintained a chiral stereostructure even after silica immobilization, though different from its structure in solution.

3.3. Chiral selectivity of aromatic enantiomers

Different chiral molecules were used for chiral recognition studies using Sil-Q_4-Cmp and Sil-Cmp as the stationary phases: enantiomers having a chiral carbon, such as benzoin and flavanone; axially chiral molecules, such as binaphthol and Tröger's base; and helical molecules (*Q* oligomers). Experiments were conducted in the reversed-phase mode. The analytical results are summarized in Table 2. Retention times on the Sil-Q_4-Cmp phase were found to increase upon adding the number of aromatic rings in the analyte. Sil-Q_4-Cmp showed chiral recognition toward Tröger's base ($\alpha_{\text{Tröger's base}}$ = 1.26, Fig. 5) but baseline separation was not achieved. For warfarin, in which two types of bulky substituents are directly bonded to the chiral center, the separation factor was 1.16, indicating a higher selectivity even though warfarin is not an axially chiral molecule. In contrast, chiral recognition was either low or absent for molecules such as α-methyl-1-naphthalene methanol and ibuprofen, in which the bond between the chiral center and the substituent is relatively easy to rotate.

To evaluate the ability of Sil-Q_4-Cmp to separate *P*- and *M*-helical quinoline oligoamide foldamers, the length of the foldamers must also be considered. The racemization (helix handedness inversion) time of a quinoline oligoamide tetramer is too short for HPLC analysis but hexamers or longer oligomers have sufficiently slow conformational dynamics to be separated [35]. Thus, we used octamers that have a racemization half-life of several hours in chloroform (at 25 °C) and much longer in protic solvents [28]. Octamers with 4-isobutoxy side chains ($Q_8{}^{i\text{Bu}}$) and with triethylene glycol

Table 2
Retention and separation factor (k and α) of Sil-Q_4-Cmp of enantiomers.

		Sil-Cmp		Sil-Q_4-Cmp	
		k	α	k	α
Atropisomers	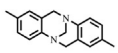	0.35	-	7.75 9.78	1.26
	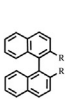 R=CH_3	2.96	-	>>65	N.D.
	=OH	0.88	-	18.28 19.55	1.07
	$=NH_2$	2.82	-	22.26 22.81	1.02
		0.39	-	13.45 14.28	1.06
	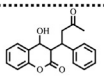	13.33	-	6.69 7.77	1.16
		0.35	-	10.50	-
		0.39	-	3.23	-
		0.39	-	3.27 3.36	1.03
		0.21	-	2.37	
	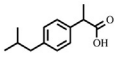	21.57	-	6.29	-
	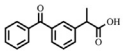	14.35	-	5.23	-

Mobile phase: MeOH/H_2O = 40/60 for Sil-Cmp, MeOH/H_2O = 50/50 for Sil-Q_4-Cmp.
Flow rate = 1.0 mLmin^{-1}. Column temperature = r.t.

Table 3
Thermodynamic parameters of Sil-Q_4-Cmp.

		$-\Delta H$ kJ/mol	$-\Delta S^*$ J/mol K	$-\Delta\Delta H$ kJ/mol	$-\Delta\Delta S$ J/mol K	$\Delta\Delta G$ (283 K) kJ/mol
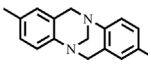	k_1	16.13	37.73	1.24	3.45	−0.82
	k_2	14.89	34.28			
$Q_8{}^{iBu}$	k_1	32.00	65.27	23.58	58.85	−14.06
	k_2	60.25	124.12			
$Q_8{}^{Tg}$	k_1	20.91	101.00	28.25	70.57	−16.86
	k_2	44.49	173.81			

Mobile phase: MeOH/H_2O = 50/50, flow rate = 1.0 ml min^{-1}.

side chains ($Q_8{}^{Tg}$) were eventually selected. Their helical structures are identical but their solubility properties differ significantly. The results indicated highly selective interactions of *P* and *M* helices with Sil-Q_4-Cmp. The separation factor was 10.35 for $Q_8{}^{iBu}$ and 14.99 for $Q_8{}^{Tg}$, showing no significant effect of the side chains despite their distinct size, flexibility, and chemical nature (Fig. 6). In addition, retention times were also similar. As such, we assumed that Sil-Q_4-Cmp did not recognize the side surface of the cylindrical foldamer but interactions took place at the top and bottom aromatic faces instead. More importantly, it was the *P*-enantiomer that showed a better interaction with the *P*-helical stationary phase, being strongly retained on the surface (Table 3).

As a control, Sil-Cmp did not show any selectivity toward any of the enantiomers and foldamers. This result agreed with the findings of Lee et al. who developed a chiral stationary phase, in which cinchonidine was immobilized onto a silica surface and showed a lack of chiral recognition [36]. Cinchonidine consists of a quincorine moiety attached to position 4 of a quinoline and its structure can be loosely compared to a quinoline monomer (*Q*) with an appended camphanyl group. Based on the results obtained with Sil-Cmp and those reported by Lee et al., one can deduce that the chiral foldamer

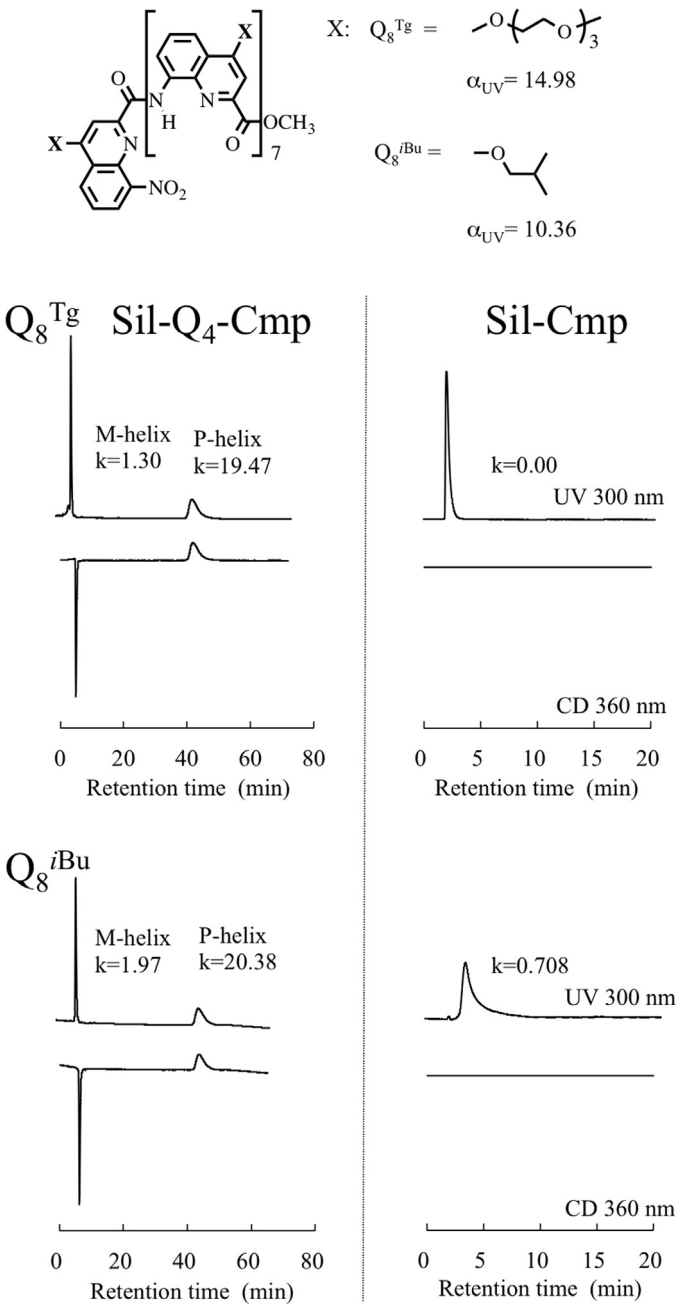

Fig. 6. Chromatograms of $Q_8{}^{iBu}$ and $Q_8{}^{Tg}$ on Sil-Q_4-Cmp and Sil-Cmp. Mobile phase: methanol, column temperature: 25 °C, flow rate: 1.0 ml min^{-1} for Sil-Q_4-Cmp, mobile phase: methanol/water = 7/3, column temperature: 25 °C, Flow rate: 1.0 ml min^{-1} for Sil-Q_4-Cmp UV wavelength: 300 nm, CD wavelength: 360 nm.

structure formed by Q_4 is directly involved in chiral recognition utilizes Sil-Q_4-Cmp.

To evaluate interactions of Sil-Q_4-Cmp with chiral analytes in the mobile phase, we used the van't Hoff equation for retention and separation factors. The correlation between the retention factor and the measured temperature is expressed by Eq. (2). Further, Eq. (3) is derived from the Gibbs–Helmholtz equation and the separation factor is the ratio of the retention factors [37]:

$$\ln k = \frac{\Delta H}{RT} + \frac{\Delta S}{R} + \ln\varphi \quad (2)$$

$$\ln\alpha = \frac{-\Delta\Delta G}{RT} = \frac{-\Delta\Delta H}{RT} + \frac{\Delta\Delta S}{R} \quad (3)$$

where ΔH and ΔS are the enthalpy and entropy change in the measurement temperature range, R is the ideal gas constant, T is the absolute temperature, and φ is the volume ratio between a stationary phase and a mobile phase; $\Delta\Delta G$, $\Delta\Delta S$, and $\Delta\Delta H$ indicate the difference in the total energy, entropy, and enthalpy between each enantiomer, respectively. The thermodynamic parameters were obtained by van't Hoff plots using Eq. (2) and Eq. (3). In addition, since the value of φ is often unknown, the intercept value of the plot is used as the estimated value, ΔS^* ($\Delta S^* = \Delta S/R + \ln\varphi$), for comparison of the entropy terms. The parameters obtained this way provided insights into the types of interactions associated with chiral recognition.

In this study, measurements were performed for $Q_8{}^{iBu}$, $Q_8{}^{Tg}$, and Tröger's base, for which high selectivity was observed between 10 and 40 °C. In this temperature range, van't Hoff plots were linear. In other words, the separation mode was constant in this temperature range, indicating that no change occurred either in the stereostructure of Cmp-Q_4 immobilized on Sil-Q_4-Cmp, or in the structure of the separated enantiomers. In addition, since $\Delta\Delta H$ and $\Delta\Delta S$ were negative in value, separation by Sil-Q_4-Cmp was enthalpy-dominated. Küster et al. discussed the chiral recognition mechanism as a function of the calculated $\Delta\Delta H$ values [37–39]. Based on their theory, if the absolute value of $\Delta\Delta$H is ≤0.1 kcal/mol (=0.4 kJ/mol), chiral recognition depends more on the chiral stereo space and the shape of the guest molecule as opposed to the static interaction. As the absolute value of $\Delta\Delta H$ increases, the intermolecular interaction effectively works on one of the enantiomers in the chiral stereo space formed by the stationary phase, thus increasing chiral recognition. If the $\Delta\Delta H$ value is larger than 0.4 kJ/mol, hydrogen bonds and π–π interactions are presumably involved. The recognition of Tröger's base by Sil-Q_4-Cmp falls into this category. Furthermore, if $\Delta\Delta H$ is larger than 1.0 kcal/mol (=4.2 kJ/mol), multiple interaction points on the stationary phase create an optimal arrangement for the stereostructure recognition of the enantiomers, resulting in high selectivity. The chiral recognition of $Q_8{}^{iBu}$ and $Q_8{}^{Tg}$ by Sil-Q_4-Cmp corresponds to this phenomenon. Given the structures of the guest and stationary phases in which most hydrogen bond donors are involved in intramolecular hydrogen bonds, and given the protic nature of the solvent, intermolecular hydrogen bonds are unlikely. Instead, aromatic stacking and the associated hydrophobic components may be responsible for the chiral separation. The fact that interactions are stronger between helices having the same handedness is reminiscent of the stacks of helical amide foldamers observed in the solid state [40,41].

4. Conclusion

In this study, we have developed a stationary phase (Sil-Q_4-Cmp) for HPLC, in which quinoline oligoamide foldamers having *P* helicity induced by an appended chiral source at the N-terminus, were immobilized on silica particles. The ability of this new stationary phase to recognize chiral molecules was examined. Spectroscopic investigations of Sil-Q_4-Cmp dispersions in solvent confirmed that Cmp-Q_4 was immobilized on the silica surface and remained chiral, but also hinted at some changes in its structure. Sil-Q_4-Cmp showed relatively high chiral recognition for axially chiral molecules such as *trans*-stilbene oxide and Tröger's base. Furthermore, Sil-Q_4-Cmp had high recognition ability for helical quinolinecarboxamide octamers, with a binding preference for helices having the same handedness as the CSP. Based on chromatographic investigations, we concluded that separation by Sil-Q_4-Cmp rests on the foldamer chiral structure and not on the appended chiral group. The results in this study represent the first known application of foldamers in chromatographic sep-

aration technology. They will certainly be useful in separating enantiomers of helically folded aromatic oligoamides in protic solvent. In water, for example, a helical octamer is kinetically inert and will not racemize over time. Purifying a one-handed enantiomer would alleviate the need to induce handedness via a covalently bound chiral group [26]. This will be advantageous for enantioselective interactions that have been identified, e.g., between helical foldamers and proteins [42] or nucleic acids [43]. However, the change in the secondary structure of quinoline oligoamide upon grafting on silica particles may vary with solvent and temperature. Thus, chromatographic conditions may have to be optimized upon changing these two parameters. Intermolecular interactions may also be tuned by changing the chemical structure of quinoline oligoamide side chains, an interface between the foldamer and guest molecules that has not been exploited in the current work. Therefore, high selectivity may be achieved via the optimization of both the foldamer's primary and secondary structures.

Acknowledgement

The authors want to gratefully acknowledge for the financial support by the "Strategic Young Researcher Overseas Visits Program for Accelerating Brain Circulation, Japan Society for the Promotion of Science".

Appendix A. Supplementary data

Supplementary data associated with this article can be found, in the online version, at http://dx.doi.org/10.1016/j.chroma.2016.01.059.

References

[1] C. Bicchi, A. D'Amato, P. Rubiolo, Cyclodextrin derivatives as chiral selectors for direct gas chromatographic separation of enantiomers in the essential oil, aroma and flavour fields, J. Chromatogr. A 843 (1999) 99–121.
[2] A. Rocco, Z. Aturki, S. Fanali, Chiral separation in food analysis, Trends Anal. Chem. 52 (2013) 206–225.
[3] V.P. Fernández, M.Á. García, M.L. Marina, Chiral separation of agricultural fungicides, J. Chromatogr. A 1218 (2011) 6561–6582.
[4] L.A. Nguyen, H. He, C.P. Huy, Chiral drugs: an overview, Int. J. Biomed. Sci. 2 (2006) 85–100.
[5] A. Shundo, M. Fukui, M. Takafuji, K. Akasaka, H. Ohrui, D. Berek, H. Ihara, Selectivity enhancement for trans-2-(2,3-anthracenedicarboximido) cyclohexane-derived diastereomers in HPLC by using an ordered organic stationary phase, Anal. Sci. 23 (2007) 311–315.
[6] J. Xie, Q. Tan, L. Yang, S. Lai, S. Tang, C. Cai, X. Chen, A simple and rapid method for chiral separation of amlodipine using dual chiral mobile phase additives, Anal. Methods 6 (2014) 4408–4413.
[7] Y. Okamoto, Chiral polymers for resolution of enantiomers, J. Polym. Sci. A 47 (2009) 1731–1739.
[8] D. Wang, J. Zhao, H. Wu, H. Wu, J. Cai, Y. Ke, X. Liang, Preparation and evaluation of novel chiral stationary phases based on quinine derivatives comprising crown ether moieties, J. Sep. Sci. 38 (2015) 205–210.
[9] C. Lin, J. Fan, W. Liu, Y. Tan, W. Zhang, H.P.L.C. Comparative, enantioseparation on substituted phenylcarbamoylated cyclodextrin chiral stationary phases and mobile phase effects, J. Pharm. Biomed. Anal. 98 (2014) 221–227.
[10] I. Ilisz, R. Berkecz, A. Péter, HPLC separation of amino acid enantiomers and small peptides on macrocyclic antibiotic-based chiral stationary phases: a review, J. Sep. Sci. 29 (2006) 1305–1321.
[11] X. Zhang, Y. Bao, K. Huang, K.L. Barnett-Rundlett, D.W. Armstrong, Evaluation of dalbavancin as chiral selector for HPLC and comparison with teicoplanin-based chiral stationary phases, Chirality 22 (2010) 495–513.
[12] V.S. Sharp, J.D. Stafford, R.A. Forbes, M.A. Gokey, M.R. Cooper, Stereoselective high-performance liquid chromatography and analytical method characterization of evacetrapib using a brush-type chiral stationary phase/A challenging isomeric separation requiring a unique eluent system, J. Chromatogr. A 1363 (2014) 183–190.
[13] H. Hettegger, M. Kohout, V. Mimini, W. Linder, Novel carbamoyl type quinine and quinidine based chiral anion exchangers implementing alkyne–azide cycloaddition immobilization chemistry, J. Chromatogr. A 1337 (2014) 85–94.
[14] S. Ray, M. Takafuji, H. Ihara, Chromatographic evaluation of a newly designed peptide-silica stationary phase in reverse phase liquid chromatography and hydrophilic interaction liquid chromatography: mixed mode behavior, J. Chromatogr. A 1266 (2012) 43–52.
[15] K. Tamura, T. Miyabe, H. Iida, E. Yashima, Separation of enantiomers on diastereomeric right- and left-handed helical poly(phenyl isocyanide)s bearing l-alanine pendants immobilized on silica gel by HPLC, Polym. Chem. 2 (2011) 91–98.
[16] A. Shundo, T. Sakurai, M. Takafuji, S. Nagaoka, H. Ihara, Molecular-length and chiral discriminations by β-structural poly(L-alanine) on silica, J. Chromatogr. A 1073 (2005) 169–174.
[17] T. Nakano, Optically active synthetic polymers as chiral stationary phases in HPLC, J. Chromatogr. A 906 (2001) 205–225.
[18] K. Ohyama, K. Oyamada, N. Kishikawa, Y. Ohba, M. Wada, T. Maki, K. Nakashima, N. Kuroda, Preparation and characterization of poly(L-phenylalanine) chiral stationary phases with varying peptide length, J. Chromatogr. A 1208 (2008) 242–245.
[19] T.H.A. Miyabe Iida Ohnishi, E. Yashima, Enantioseparation on poly(phenyl isocyanide)s with macromolecular helicity memory as chiral stationary phases for HPLC, Chem. Sci. 3 (2012) 863–867, as Chiral Stationary Phases for HPLC, Chem. Lett., 41 (2012) 809-811.
[20] K. Shimomura, T. Ikai, S. Kanoh, E. Yashima, K. Maeda, Switchable enantioseparation based on macromolecular memory of a helical polyacetylene in the solid state, Nat. Chem. 6 (2014) 429–434.
[21] G. Guichard, I. Huc, Synthetic foldamers, Chem. Commun. 47 (2011) 5933–5941.
[22] I. Saraogi, A.D. Hamilton, Recent advances in the development of aryl-based foldamers, Chem. Soc. Rev. 38 (2009) 1726–1743.
[23] D.J. Hill, M.J. Mio, R.B. Prince, T.S. Hughes, J.S. Moore, Field guide to foldamers, Chem. Rev. 101 (2001) 3893–4011.
[24] S.H. Gellman, Foldamers: a manifesto, Acc. Chem. Res. 31 (1998) 173–180.
[25] T. Qi, T. Deschrijver, I. Huc, Large-scale and chromatography-free synthesis of an octameric quinoline-based aromatic amidehelical foldamer, Nat. Protoc. 8 (2013) 693–708.
[26] C. Dolain, A. Grélard, M. Laguerre, H. Jiang, V. Maurizot, I. Huc, Solution structure of quinoline- and pyridine-derived oligoamide foldamers, Chem. Eur. J. 11 (2005) 6135–6144.
[27] H. Jiang, J.M. Léger, I. Huc, Aromatic δ-peptides, J. Am. Chem. Soc. 125 (2003) 3448–3449.
[28] T. Qi, V. Maurizot, H. Noguchi, T. Charoenraks, B. Kauffmann, M. Takafuji, H. Ihara, I. Huc, Solvent dependence of helix stability in aromatic oligoamide foldamers, Chem. Commun. 48 (2012) 6337–6339.
[29] A.M. Kendhale, L. Poniman, Z. Dong, K. Laxmi-Reddy, B. Kauffmann, Y. Ferrand, I. Huc, Absolute control of helical handedness in quinoline oligoamides, J. Org. Chem. 76 (2011) 195–200.
[30] S.J. Dawson, Aí. Meíszaíros, L. Pethő, C. Colombo, A. Cseíkei, I. Huc, Controlling helix handedness in water-soluble quinoline oligoamide foldamers, Eur. J. Org. Chem. 20 (2014) 4265–4275.
[31] G.E. Berendsen, K.A. Pikaart, L. de Galan, Preparation of various bonded phases for HPLC using monochlorosilanes, J. Liq. Chromatogr. 3 (1980) 1437–1464.
[32] M. Kubasik, A. Brown, Acceleration of short helical peptide conformational dynamics by trifluoroethanol in an organic solvent, ChemBioChem 6 (2005) 1187–1190.
[33] N. Ousaka, T. Sato, R. Kuroda, Intramolecular crosslinking of an optically inactive 3_{10}-helical peptide: stabilization of structure and helix sense, J. Am. Chem. Soc. 130 (2008) 463–465.
[34] J. Garric, J.M. Leger, A. Grelard, M. Ohkita, I. Huc, Solid state and solution conformation of 2-pyridinecarboxylic acid hydrazides: a new structural motif for foldamers, Tetrahedron Lett. 44 (2003) 1421–1424.
[35] N. Delsuc, T. Kawanami, J. Lefeuvre, A. Shundo, H. Ihara, M. Takafuji, I. Huc, Kinetics of helix-handedness inversion: folding and unfolding in aromatic amide oligomers, ChemPhysChem 9 (2008) 1882–1890.
[36] Y. Lee, K. Yamashita, M. Eto, K. Onimura, H. Tsutsumi, T. Oishi, Synthesis of novel chiral poly(methacrylate) s bearing urethane and cinchona alkaloid moieties in side chain and their chiral recognition abilities, Polymer 43 (2002) 7539–7547.
[37] E. Küsters, V. Loux, E. Schmid, Enantiomeric separation of chiral sulphoxides: Screening of cellulose-based sorbents with particular reference to cellulose tribenzoate, J. Chromatogr. A 666 (1994) 421–432.
[38] Y. Zhang, S. Bai, B. Song, P.S. Bhadury, D. Hu, S. Yang, X. Zhang, H. Fan, P. Lu, Enantio separation and plant virucidal bioactivity of new quinazoline derivatives with α-aminophosphonate moiety, J. Chromatogr. B 878 (2010) 1285–1289.
[39] X. He, R. Lin, H. He, M. Sun, D. Xiao, Chiral separation of ketoprofen on a chirobiotic T column and its chiral recognition mechanisms, Chromatographia 75 (2012) 1355–1363.
[40] H. Zhao, W.Q. Ong, F. Zhou, X. Fang, X. Chen, S.Y. Li, H. Su, N.J. Cho, H. Zeng, Chiral crystallization of aromatic helical foldamers via complementarities in shape and end functionalities, Chem. Sci. 3 (2012) 2042–2046.
[41] D. Haldar, H. Jiang, J.M. Léger, I. Huc, Double versus single helical structures of oligopyridine–dicarboxamide strands. Part 2: the role of side chains, Tetrahedron 63 (2007) 6322–6330.
[42] J. Buratto, C. Colombo, M. Stupfel, S.J. Dawson, C. Dolain, B.L. d'Estaintot, L. Fischer, T. Granier, M. Laguerre, B. Gallois, I. Huc, Structure of a complex formed by a protein and a helical aromatic oligoamide foldamer at 2.11 Å resolution, Angew. Chem. Int. Ed. 53 (2014) 883–887.
[43] L. Delauriére, Z. Dong, K. Laxmi-Reddy, F. Godde, J.J. Toulmé, I. Huc, Deciphering aromatic oligoamide foldamer–DNA interactions, Angew. Chem. Int. Ed. 51 (2012) 473–477.